Letter

Role of Coulomb interaction in the phase formation of fcc Ce: Correlation matrix renormalization theory

Jun Liu,[1] Yongxin Yao,[1,2] Jianhua Zhang,[2] Kai-Ming Ho,[1,2] and Cai-Zhuang Wang[1,2,*]
[1]*Ames Laboratory, U.S. Department of Energy, Iowa State University, Ames, Iowa 50011, USA*
[2]*Department of Physics and Astromany, Iowa State University, Ames, Iowa 50011, USA*

(Received 10 February 2021; revised 30 June 2021; accepted 6 August 2021; published 30 August 2021)

The effect of electronic Coulomb interaction on the phase formation of fcc Ce lattice is investigated by full *ab initio* calculations without adjustable Coulomb U and J parameters using the Gutzwiller wavefunction-based correlation matrix renormalization theory (CMRT). Its total energy and pressure as a function of volume agree reasonably well with existing DFT + Gutzwiller calculations and experiments, indicating correct capture of electronic correlation and screening effects within the CMRT formalism. A stable phase is found in line with the experimental α-Ce phase, and a lurking phase is identified supposedly linked with the experimental γ-Ce phase. A criterion based on the local $4f$ electron charge fluctuation is introduced to confirm the distinct electronic correlation natures of both phases.

DOI: 10.1103/PhysRevB.104.L081113

Introduction. Cerium (Ce) has a rich phase diagram particularly featured by the α-Ce and γ-Ce phases in the fcc crystal structure. Under ambient pressure, these two phases take turns to be the stable structure at low and high temperatures. At room temperature, increasing pressure might lead to an isostructural first-order phase transition from γ-Ce to α-Ce with a sudden volume collapse (VC) of about 15% which ends at a critical point with its critical volume denoted as V_c on the temperature-pressure (T-P) phase diagram [1]. Both a Bremsstrahlung isochromat and photoemission spectroscopy of $4f$ electrons recorded a spectral weight suppression on γ-Ce but a resonance peak on α-Ce [2–4] at their Fermi levels. A peak around 2 eV below the Fermi energy was shared by both phases [5]. This was understood to be the lower Hubbard band reflecting the correlated nature of both Ce phases [6] with γ-Ce being more correlated given a more concentrated $4f$ Fock state occupation [7]. Infrared optical spectroscopy and neutron scattering, on the other hand, showed little difference between the two phases except around 300 meV [8,9], where a small difference arises attributed to spin-orbit coupling (SOC), hinting at its relevant role played in both phases. For magnetic susceptibility, α-Ce exhibits a Pauli-like behavior, while γ-Ce shows a Curie-Weiss behavior with a small local moment [10]. Lattice vibration plays a controversial role in both phases [11,12], and the phonon density of state changes little across the VC transition [12]. In all, experimental evidence has suggested that the abrupt change between α-Ce and γ-Ce is mainly due to electron correlations in the Ce lattice.

A plethora of theoretical studies have been carried out to interpret the physics underneath both Ce phases. The key role played by correlated $4f$ electrons and the very change in nature from local to nonlocal $4f$ electrons across the VC transition are widely accepted, and how they participate in the phase formation and transition has been proposed in a variety of models [13–15]. While *ab initio* density functional theory (DFT) embedding methods [16] such as DFT + dynamical mean field theory (DFT + DMFT), DFT + Gutzwiller (DFT + G), and DFT + U [17–19] have confirmed the importance of appropriately treating the local electronic correlation of $4f$ electrons, they rely on adjustable Coulomb interaction U and J parameters which cause concerns about their predictive power. There have also been *ab initio* calculations that have not incurred adjustable energy parameters [20–22]. However, a comprehensive understanding and in-depth exploration of the role of Coulomb interactions in fcc Ce lattices have not been provided.

In this Letter, we concentrate on possible consequences the $4f$ electron might have with its electronic Coulomb interaction on fcc Ce lattice using a recently developed fully *ab initio* method, the correlation matrix renormalization theory (CMRT) [24–26]. Differing from existing *ab initio* DFT embedding studies, CMRT works directly with bare Coulomb interactions, which readily gives us the power to carefully study the role of electronic Coulomb interactions in this system and to seek possible physics beyond what is already known. Our calculation produces a stable state nearby α-Ce and presents evidence on a possible lurking phase located at the strongly correlated region where γ-Ce sits.

Method. CMRT is a fully *ab initio* variational theory specifically designed for strongly correlated electron systems by taking a multiband Gutzwiller wave function as its trial wave function. The overall formalism was fully derived in Ref. [26] and is briefly outlined below. By assuming one atom per unit cell, the CMRT total energy is

$$E_{\text{total}} = \sum_{\substack{ij \\ \alpha\beta,\,\sigma}} t_{i\alpha,j\beta}\langle c^{\dagger}_{i\alpha\sigma} c_{j\beta\sigma}\rangle + \frac{1}{2}\sum_{\substack{ijkl \\ \alpha\beta\gamma\delta,\,\sigma\sigma'}} U^{\alpha\beta\gamma\delta}_{ijkl}\langle\langle c^{\dagger}_{i\alpha\sigma} c_{k\gamma\sigma}\rangle\langle c^{\dagger}_{j\beta\sigma'} c_{l\delta\sigma'}\rangle$$

*wangcz@ameslab.gov

$$- \delta_{\sigma\sigma'} \langle c^\dagger_{i\alpha\sigma} c_{l\delta\sigma'} \rangle \langle c^\dagger_{j\beta\sigma'} c_{k\gamma\sigma} \rangle)$$
$$+ \sum_i \sum_\Gamma E_{i\Gamma} (p_{i\Gamma} - p_{i\Gamma_0}), \quad (1)$$

with $ijkl$ sites, $\alpha\beta\gamma\delta$ orbitals, $\sigma\sigma'$ spins, and Γ Fock states in the local correlated subspace $\mathcal{C}$. The energy parameters, $t_{i\alpha,j\beta}$, $U^{\alpha\beta\gamma\delta}_{ijkl}$, and $E_{i\Gamma}$, represent bare hopping, Coulomb integrals, and eigenvalues of a local Hamiltonian defined in $\mathcal{C}$ and with number operators only. The first two terms in Eq. (1) give the CMRT expectation value of the bare lattice Hamiltonian with two-body interactions expanded via Wick's theorem in its lowest-order approximation in terms of a one-body term. Specifically, this one body term is related to its noninteracting counterpart through

$$\langle c^\dagger_{i\alpha\sigma} c_{i\beta\sigma} \rangle = f(z_{\alpha\sigma}) f(z_{\beta\sigma}) \langle c^\dagger_{i\alpha\sigma} c_{i\beta\sigma} \rangle_0 + [1 - \delta_{\alpha\beta} f^2(z_{\alpha\sigma})] n^0_{i\alpha\sigma}. \quad (2)$$

Here, $f(z_{\alpha\sigma})$ is inferred from an exactly solvable model with $z_{\alpha\sigma}$ being the Gutzwiller renormalization factor [25]. To best preserve dominant local physics, the CMRT replaces the approximate local energy with its rigorous value through the third term in Eq. (1) involving $p_{i\Gamma}$ and $p_{i\Gamma_0}$ as full and noninteracting Fock state probabilities. One major error source in E_{total} is with its Fock terms. This error is carefully addressed by adding to the bare Hamiltonian a commuting null sum rule Hamiltonian designed based on total charge conservation. This extra Hamiltonian aims at best canceling out accumulative Fock contributions and meanwhile redistributing a portion of nonlocal direct Coulomb interactions to local sites for a rigorous treatment. The variational minimization of E_{total} results in a Gutzwiller equation set to be self-consistently solved, which is capable of producing results quantitatively comparable to experiments in weakly correlated lattice systems [26].

In this study, CMRT calculations are interfaced with the Hartree-Fock (HF) module of the Vienna *Ab Initio* Simulation Package (VASP) [27] to update the effective single-electron Hamiltonian and its eigenspectrum based on the interacting charge density and correlated renormalization factors produced by solving the Gutzwiller equation set in a self-consistent procedure [26]. We focus on the nonmagnetic state without SOC and perform all the CMRT calculations using quasi-atomic minimal basis set orbitals (QUAMBOs) constructed from LDA calculations [28] and with a pseudopotential defined with the projector-augmented wave method [29] and the exchange-correlation of the Ceperley-Alder [30] form. The validity of QUAMBOs for CMRT has been verified in previous publications [24–26]. The use of QUAMBOs endows CMRT with a computational speed of a minimal basis HF calculation, which is very efficient for strongly correlated systems. Brillouin zone sampling is done by VASP with an automatically generated K-point grid taking a R_k length of 50 ($R_k = 50$) [31].

Results. We present E-V curves from nonmagnetic HF, DFT + G, and CMRT calculations in Fig. 1. These methods are closely related, and their differences in total energy reflect the efficacy of CMRT in treating correlated electron systems. CMRT constructs its single-particle secular equations on top of a noninteracting HF Hamiltonian. Consequently, CMRT total energy includes the exact exchange energy with its dominant local components replaced with an exact local energy. These actions significantly change the HF behavior and reassuringly shift the stable phase from beyond γ-Ce, which is likely an artifact of the weak interacting HF method, back to nearby α-Ce in CMRT. This very fact shows the design of CMRT serves its purpose of appropriately treating (static) correlation effects well. CMRT and DFT + G share many things in common [18,26], but have one key difference in how they represent electronic screening effects. Intimately connected with and thus sharing close performance with DFT + DMFT [18], DFT + G is based on a DFT energy functional where electronic correlation is partially accounted for with an exchange-correlation functional. DFT + G further replaces its local energy component with a supposedly more accurate term evaluated with a tight-binding Hamiltonian defined with a set of screened U and J effective energy parameters which can be adjusted to best match experiments. CMRT, however, works with bare Coulomb interactions throughout the whole calculation. Electronic screening is automatically included through an iterative interacting charge density update by solving the Gutzwiller equation set in CMRT with a self-consistent procedure. Such screening effects influence the correlation-renormalized hoppings and optimized local correlated Fock occupation, etc. The total energies obtained by both CMRT and DFT + G are shown in Fig. 1. Their close similarity substantiates a correct capture of the electronic screening effect in this system within CMRT. This agreement might also validate the use of $U = 6$ eV [23] in DFT + G on the fcc Ce lattice.

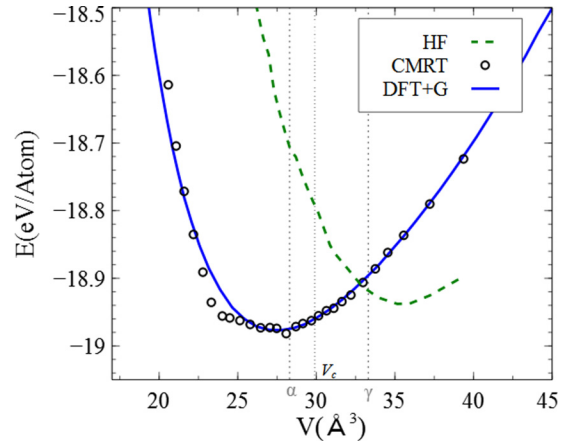

FIG. 1. E-V curves on fcc Ce calculated with nonmagnetic HF, DFT + G with $U = 6$ eV (upper right panel of Fig. 1 in Ref [23]), and CMRT. Taking CMRT energy as the reference, arbitrary vertical energy shift are applied to HF and DFT + G for a best comparison with CMRT.

P-V curves are shown in Fig. 2 to compare CMRT with experiments [32,33] and DFT + G [23] acting as the 0 K reference. As can be seen, the CMRT pressure evaluated with finite difference passes $P = 0$ GPa roughly at α-Ce with little volume dependence halfway between the α- and γ-Ce phases. It agrees reasonably well in the overall trend with DFT + G throughout the whole volume range except for nearby 25 Å^3, likely due to systematic error inherent in the basis set used here.

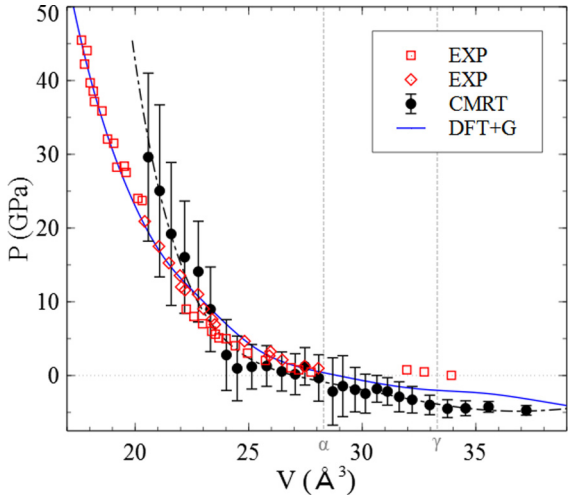

FIG. 2. The P-V data obtained from CMRT are compared against experiments [32,33]. DFT + G at $U = 6$ eV with SOC [23] is also included as the 0 K pressure reference. Error bars of CMRT pressure are derived from those in total energy calculation, see Supplemental Material Ref. [34].

Figure 3 possibly hints at different physics coming out of the fcc Ce lattice under the mere effect of electronic hopping and Coulomb interactions. The CMRT E-V curve in Fig. 3(a) might suggest the existence of more than just a

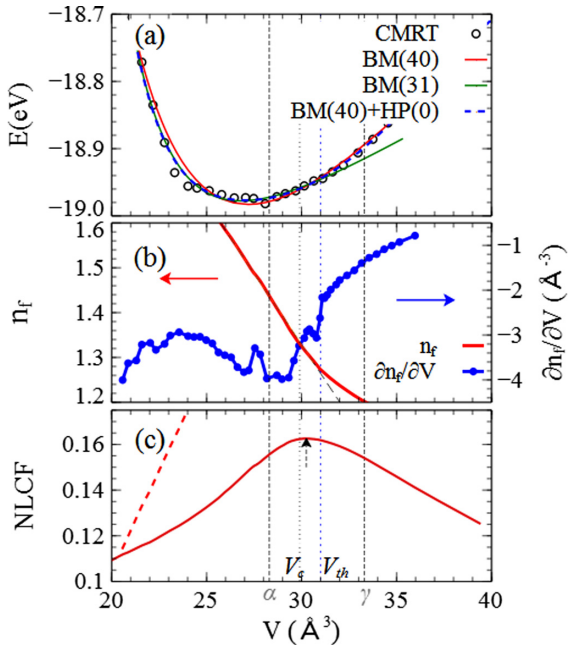

FIG. 3. (a) CMRT E-V curve and its different equation of state fits, including a BM(40) + HP(0) fit over the whole volume range within 40 Å^3 and two BM fits in solid red over the same volume range and solid green for less than V_{th}. (b) Volume dependence of n_f (solid red, left axis) and $\partial n_f/\partial V$ (dotted solid blue, right axis), as well as a linear fit (dashed black) over part of n_f to show the relevant irregularities in $\partial n_f/\partial V$ are due to error. (c) Volume dependence of NLCF (solid red) and its weak interacting limit, $1/n_f$ (dashed red), down-shifted to give contrast against CMRT. The middle two vertical lines denote V_c and V_{th}, respectively, and the arrow in panel (c) denotes V_{TP}.

stable phase. The CMRT energies within a reasonable volume V covering both Ce phases were fitted with a series of nested models formed by the Birch-Murnaghan equation of state (BM) [35] plus an nth-order Hermite Polynomial (HP), written in a shorthand notation as BM(V) + HP(n). These models are statistically judged using the Akaike information criterion with a correction for small sample sizes (AICc) [36], with the lowest AICc score designating the optimal fit, which best balances between the number of fitting parameters and the residual error. Specifically in this work, the best fit, BM(40) + HP(0), gives an equilibrium volume of $\tilde{V}_\alpha = 27$ Å^3 and a corresponding bulk modulus of $\tilde{B}_0 = 21$ GPa, quite close to 27.9 Å^3 and 20 GPa of α-Ce [32]. In contrast, BM(40) itself shows perceivable differences from the optimal fit and fails to reproduce the overly flat energy basin of the CMRT energies. Since the Birch-Murnaghan equation of state is perturbatively derived from the elastic theory of a single phase with changing volume [35,37], its insufficiency to express a set of E-V data supposedly suggests these data are not from a single phase. Thus, the statistical analysis hints at hidden information, which is further analyzed with total $4f$ electron occupation, n_f, and its numerical derivative, $\partial n_f/\partial V$, both shown in Fig. 3(b). Given less noisy n_f, $\partial n_f/\partial V$ is capable of showing a clear jump at a threshold volume of $V_{th} = 31$ Å^3. Such a sudden change in slope of n_f might signalize the onset of a nonadiabatic change in the spatial charge distribution possibly due to single-particle level crossing. Repeating the model selection procedure on the E-V data within V_{th} returns BM(V_{th}) as the best fit, which nearly overlaps with BM(40) + HP(0) but deviates away beyond V_{th} as shown in Fig. 3(a). The combined message here is energy data less than V_{th} could be understood with one phase but such a conclusion becomes less clear beyond V_{th}. We might further establish an intimate connection between the mysterious region and γ-Ce by looking into the *normalized* local charge fluctuation (NLCF) for $4f$ electrons, $\langle \delta n_f^2 \rangle / n_f^2 = \langle \hat{n}_f^2 \rangle / n_f^2 - 1$, which varies as $1/n_f$ in the weak interacting limit. It presumably increases when the lattice constant is small as inferred from Fig. 3(b), but it must decay in the strong correlation limit as the local charge fluctuation gets increasingly suppressed. This should result in a bell shape as volume increases, as clearly seen in Fig. 3(c) with the turning point volume V_{TP} marking the dividing line of the qualitatively different correlation nature of $4f$ electrons in fcc Ce. CMRT correctly puts a stable phase in the less correlated region, supposedly the experimental α-Ce phase, and develops something unknown at V_{th} in the strongly correlated region not far from V_γ. We might call it a lurking phase as it is not yet stable but might be further stablized with spin degrees of freedom included in the calculation, as suggested by DFT + U and DFT + G [23,38].

Discussion. Motivated by the literature review that a physical stable phase and its total energy related properties mainly depend on a proper treatment of the local correlated $4f$ electronic interactions on the fcc Ce lattice, we apply our recently proposed fully *ab initio* CMRT to study the possible physics out of the electronic Hamiltonian in a nonmagnetic state. Compared against HF and DFT + G, CMRT is shown to properly treat electronic correlation effects and naturally render the proper amount of screening within its formalism starting from bare Coulomb interactions. These observations help to validate CMRT as a feasible fully *ab initio* method

for strongly correlated electron systems. On the other hand, the close comparison between DFT + G [23] and CMRT given here should by no means be used to judge the quality of CMRT on the isostructural VC phase transition in fcc Ce lattice as SOC is not treated in CMRT here.

The introduction of NLCF helps to establish an intimate connection between the lurking phase suggested here and γ-Ce. It might be interesting to further understand how NLCF helps to delineate the changing nature of electronic correlation in this system. Obviously, such a change must be related with electronic kinetic and Coulomb potential energies, the only two energies treated in this study. Physically, a reduced volume renders enhanced hopping and hybridization which might overcome intersite Coulomb repulsion and bring $4f$ electrons out of its localized states to interact more actively with itinerant electrons. Such a delicate competition brings up a stable phase around V_α in CMRT. Based on the same trend shared by its CMRT and $1/n$ limiting behaviors, NLCF tells us that this phase is less correlated with kinetic energy dominating Coulomb potential energy and gives $4f$ electrons a tendency to move around, or be nonlocal. Beyond V_{TP}, Coulomb repulsions take over kinetic energy, thus preventing $4f$ electrons from moving around, viz., being local. Located within this region, γ-Ce is thus correctly predicted to be strongly correlated by CMRT. V_{TP} might be an estimator for the critical volume V_c by noting this is where α-Ce joins γ-Ce, say, on the P-V phase diagram at the critical temperature. The nearly identical values between V_{TP} and V_c support the objectivity of this study. In the above analysis, NLCF plays an indicating role of how correlation affects electronic behavior in the fcc Ce lattice. The local-nonlocal physics indicated by NLCF in fcc Ce is consistent with other theoretical and experimental studies [7,15]. In weakly correlated systems, NLCF is expectedly less informative [39].

Acknowledgments. This work was supported by the U.S. Department of Energy (DOE), Office of Science, Basic Energy Sciences, Materials Science and Engineering Division, including the computer time support from the National Energy Research Scientific Computing Center (NERSC) in Berkeley, CA. The research was performed at Ames Laboratory, which is operated for the U.S. DOE by Iowa State University under Contract No. DEAC02-07CH11358.

[1] D. C. Koskenmaki and J. K. A. Gschneidner, in *Handbook on the Physics and Chemistry of Rare Earths*, edited by J. K. A. Gschneidner and L. Eyring (Elsevier, Amsterdam, 1978), Vol. 1, Chap. 4.
[2] E. Wuilloud, H. R. Moser, W. D. Schneider, and Y. Baer, Phys. Rev. B **28**, 7354 (1983).
[3] F. Patthey, B. Delley, W. D. Schneider, and Y. Baer, Phys. Rev. Lett. **55**, 1518 (1985).
[4] L. Z. Liu, J. W. Allen, O. Gunnarsson, N. E. Christensen, and O. K. Andersen, Phys. Rev. B **45**, 8934 (1992).
[5] D. M. Wieliczka, C. G. Olson, and D. W. Lynch, Phys. Rev. B **29**, 3028 (1984).
[6] B. Amadon, S. Biermann, A. Georges, and F. Aryasetiawan, Phys. Rev. Lett. **96**, 066402 (2006).
[7] J.-P. Rueff, J.-P. Itié, M. Taguchi, C. F. Hague, J.-M. Mariot, R. Delaunay, J.-P. Kappler, and N. Jaouen, Phys. Rev. Lett. **96**, 237403 (2006).
[8] J. W. van der Eb, A. B. Kuz'menko, and D. van der Marel, Phys. Rev. Lett. **86**, 3407 (2001).
[9] A. P. Murani, Z. A. Bowden, A. D. Taylor, R. Osborn, and W. G. Marshall, Phys. Rev. B **48**, 13981 (1993).
[10] A. V. Nikolaev and A. V. Tsvyashchenko, Phys.-Usp. **55**, 657 (2012).
[11] M. Krisch, D. L. Farber, R. Xu *et al.*, Proc. Natl. Acad. Sci. USA **108**, 9342 (2011).
[12] M. E. Manley, R. J. McQueeney, B. Fultz, T. Swan-Wood, O. Delaire, E. A. Goremychkin, C. J. Cooley, W. L. Hults, J. C. Lashley, R. Osborn, and J. L. Smith, Phys. Rev. B **67**, 014103 (2003).
[13] L. Pauling, J. Am. Chem. Soc. **69**, 542 (1947).
[14] J. W. Allen and R. M. Martin, Phys. Rev. Lett. **49**, 1106 (1982).
[15] B. Johansson, I. A. Abrikosov, M. Aldén, A. V. Ruban, and H. L. Skriver, Phys. Rev. Lett. **74**, 2335 (1995).
[16] U. Mordovina, T. E. Reinhard, I. Theophilou, H. Appel, and A. Rubio, J. Chem. Theory Comput. **15**, 5209 (2019).
[17] A. Georges, G. Kotliar, W. Krauth, and M. J. Rozenberg, Rev. Mod. Phys. **68**, 13 (1996).
[18] N. Lanatà, Y. Yao, C.-Z. Wang, K.-M. Ho, and G. Kotliar, Phys. Rev. X **5**, 011008 (2015).
[19] A. I. Liechtenstein, V. I. Anisimov, and J. Zaanen, Phys. Rev. B **52**, R5467 (1995).
[20] A. Svane, Phys. Rev. B **53**, 4275 (1996).
[21] M. Casadei, X. Ren, P. Rinke, A. Rubio, and M. Scheffler, Phys. Rev. Lett. **109**, 146402 (2012).
[22] N. Devaux, M. Casula, F. Decremps, and S. Sorella, Phys. Rev. B **91**, 081101(R) (2015).
[23] N. Lanatà, Y.-X. Yao, C.-Z. Wang, K.-M. Ho, J. Schmalian, K. Haule, and G. Kotliar, Phys. Rev. Lett. **111**, 196801 (2013).
[24] C. Liu, J. Liu, Y. X. Yao, P. Wu, C. Z. Wang, and K. M. Ho, J. Chem. Theory Comput. **12**, 4806 (2016).
[25] X. Zhao, J. Liu, Y.-X. Yao, C.-Z. Wang, and K.-M. Ho, Phys. Rev. B **97**, 075142 (2018).
[26] J. Liu, X. Zhao, Y. Yao, C.-Z. Wang, and K.-M. Ho, J. Phys.: Condens. Matter **33**, 095902 (2021).
[27] G. Kresse and J. Furthmüller, Phys. Rev. B **54**, 11169 (1996).
[28] X. Qian, J. Li, L. Qi, C.-Z. Wang, T.-L. Chan, Y.-X. Yao, K.-M. Ho, and S. Yip, Phys. Rev. B **78**, 245112 (2008).
[29] G. Kresse and D. Joubert, Phys. Rev. B **59**, 1758 (1999).
[30] D. M. Ceperley and B. J. Alder, Phys. Rev. Lett. **45**, 566 (1980).
[31] See Supplemental Material at http://link.aps.org/supplemental/10.1103/PhysRevB.104.L081113 for K-point grid convergence.
[32] J. Olsen, L. Gerwardi, U. Benedicti, and J. Itie, Physica B+C (Amsterdam) **133**, 129 (1985).

[33] W. Zachariasen and F. Ellinger, Acta Crystallogr., Sect. A: Cryst. Phys., Diffr., Theor. Gen. Crystallogr. **33**, 155 (1977).
[34] See Supplemental Material at http://link.aps.org/supplemental/10.1103/PhysRevB.104.L081113 for CMRT total energy error estimation.
[35] F. D. Murnaghan, Proc. Natl. Acad. Sci. USA **30**, 244 (1944).
[36] J. E. Cavanaugh, Stat Probab. Lett. **33**, 201 (1997).
[37] T. Katsura and Y. Tange, Minerals **9**, 745 (2019).
[38] Y. Wang, L. G. Hector, H. Zhang, S. L. Shang, L. Q. Chen, and Z. K. Liu, Phys. Rev. B **78**, 104113 (2008).
[39] See Supplemental Material at http://link.aps.org/supplemental/10.1103/PhysRevB.104.L081113 for a typical illustration.